July 2026

A Study of Nonlinear Dynamics

Syeda Nialish Fatima and Fasiha Shoukat

Physlab, Syed Babar Ali School of Science and Engineering,
Lahore University of Management Sciences, Lahore, Pakistan

Abstract

This study investigates the generation of electronic chaos using a simplified third-order jerk system based on the foundational framework of J. C. Sprott. The circuit utilizes standard components like operational amplifiers and resistors, avoiding complex analog multipliers or inductors like in Chua's Circuit. All four nonlinear $G(x)$ configurations were tested in LTspice using DC sweep analysis to verify their characteristic curves. Transient simulations successfully demonstrated chaotic attractor dynamics. Additionally, parameter sweeps on resistor R_{10} showed how tuning resistance controls the size and stability of the attractor.

1 Introduction

Most physical systems are modeled linearly, meaning outputs scale directly with inputs for easy prediction. Nonlinear systems violate this proportional rule, producing complex outcomes that linear methods fail to anticipate. Chaos represents an extreme form of nonlinearity. Although governed by strict equations, chaotic systems remain entirely unpredictable due to extreme sensitivity to initial conditions. Traditionally, Chua's circuit served as the primary electronic model for studying this behavior using specialized hardware and complex components.

To address these limitations, following J. C. Sprott's framework and his paper, "A new class of chaotic circuit," this report explores electronic chaos through a streamlined third-order jerk system using standard components like resistors, capacitors, diodes, and operational amplifiers analyzed via LTspice simulations. At the core of the mathematical model is a third-order ordinary differential equation known as a jerk equation:

$$\dddot{x} + A\ddot{x} + \dot{x} = G(x). \tag{1}$$

In equation (1), $G(x)$ represents a nonlinear function. The main circuit shown in Fig. 1 acts as the core system to solve the third-order differential equation. It uses three active operational amplifiers as integrators connected together with standard resistors and capacitors. The output of this loop feeds into a nonlinear block labeled $G(x)$, which then loops back into the circuit to generate chaotic behavior.

Parameter A is damping set by a feedback resistor in the first lossy integrator stage and remains constant across all circuits. Parameter B controls the slope of the nonlinear pushback via diode branches and resistor values. Parameter C is a constant offset from a fixed-supply branch that changes attractor size, not shape. Variable x is a real node voltage at the third integrator output defined by circuit topology rather than a pre-existing physical quantity.

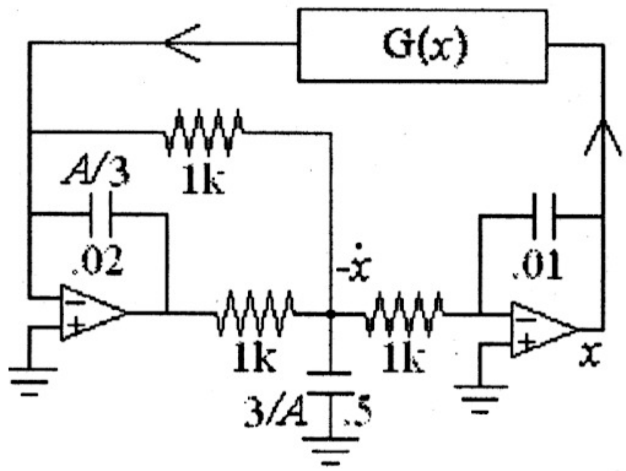

Figure 1: The general jerk-equation circuit. $G(x)$ (top) is the nonlinear feedback element; the left op-amp is a damped integrator; the central passive network labelled $-\dot{x}$ is a passive RC stage; the right op-amp is a clean integrator producing the output x.

2 Mathematical modeling

Before deriving anything circuit-specific, it is worth tracing why Sprott's equation looks the way it does. The Poincaré–Bendixson theorem states that a continuous-flow system needs at least three dynamical variables and at least one nonlinearity to exhibit chaos [2]. Two-variable continuous systems can only produce fixed points, limit cycles, or divergence, never chaos. Any three-variable system with a single nonlinearity can be rewritten as one third-order ordinary differential equation in a single scalar variable x:

$$\dddot{x} = F(\ddot{x}, \dot{x}, x). \tag{2}$$

$\dddot{x}$ (the derivative of acceleration) is called jerk in mechanics; such equations are called jerk equations [3]. Sprott's earlier work searched for the simplest possible dissipative quadratic jerk equation and found:

$$\dddot{x} = -A\ddot{x} + \dot{x}^2 - x, \tag{3}$$

which is chaotic for $A \gtrsim 2.017$. Replacing the quadratic nonlinearity with an absolute-value term $|\dot{x}|$ fails to produce chaos for any A. However, using $|x|$ instead of $|\dot{x}|$ yields chaos:

$$\dddot{x} = -A\ddot{x} - \dot{x} + |x| - 1, \tag{4}$$

chaotic for $A \gtrsim 0.6$. Generalizing the function $|x| - 1$ to a suitably shaped nonlinear function gives the general form used in this paper, Eq. (1). Chua's circuit showed that chaos can be built in hardware, but it needs an inductor, which is bulky and hard to use. Equation (5) avoids inductors completely. It uses simple diodes and resistors to build $G(x)$, making the circuit cheaper, smaller, and much easier to build.

The circuit consists of three main functional stages as shown in Fig. 1. First, the left op-amp's inverting input receives feedback current directly from the $G(x)$ block, which is held at virtual ground (0 V). The feedback network for this stage consists of a 1 kΩ resistor in parallel with a capacitor labeled $A/3$, $0.02\,\mu$F for $A = 0.6$, forming a summing integrator that establishes the system damping A.

Second, the central node labeled $-\dot{x}$ is connected to the left op-amp's output ($\ddot{x}$) via a 1 kΩ resistor and feeds back to its inverting input through another 1 kΩ resistor. This node is shunted to ground through a capacitor labeled $3/A$, $0.5\,\mu$F for $A = 0.6$, forming a passive RC network that replaces a third active op-amp integrator. Finally, the right op-amp acts as an active integrator with a 1 kΩ input resistor and a $0.01\,\mu$F feedback capacitor. Its output represents state variable x, which is probed for measurement and fed back into the $G(x)$ block to close the loop.

3 Simulations and results

Circuit (a): $G(x) = B|x| - C$

Two parallel paths connect input to output. A direct path through resistor $1/2B$ ($5000\,\Omega$) combines with a diode-clamped path (featuring resistors $1/6B$ ($1667\,\Omega$) and $1/3B$ ($3333\,\Omega$) with an op-amp and diode stage) to process the input signal symmetrically. A third branch, resistor V_0/C ($45\,\text{k}\Omega$) in series with reference $V_0 = 9\,\text{V}$, injects a constant current $-C$ independent of x:

$$G(x) = B|x| - C. \tag{5}$$

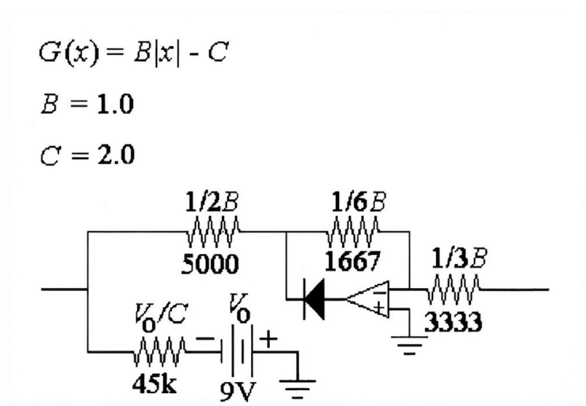

(a)

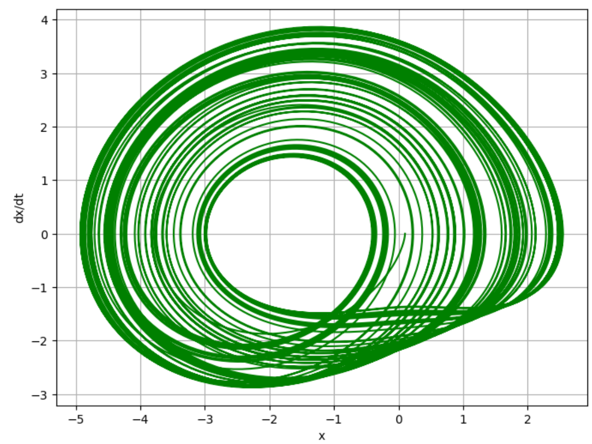

(b)

Figure 2: Python simulation of the chaotic attractor in the $x - \dot{x}$ plane for $G(x) = B|x| - C$.

Circuit (b): $G(x) = -B\max(x, 0) + C$

A single diode-clamp branch: resistor $1/B$ ($1667\,\Omega$), a $1\,\text{k}\Omega$ resistor into an op-amp, a diode, and a further $1\,\text{k}\Omega$ resistor to the output carry all the x-dependent current, with no bypass path. For $x \leq 0$, the diode is reverse-biased, and the branch contributes 0; for $x > 0$, it conducts and contributes $-Bx$. A constant-offset branch (resistor $V_0/C = 180\,\text{k}\Omega$, $V_0 = 9\,\text{V}$, supply polarity reversed relative to circuit (a)) adds $+C$ unconditionally:

$$G(x) = -B\max(x, 0) + C. \tag{6}$$

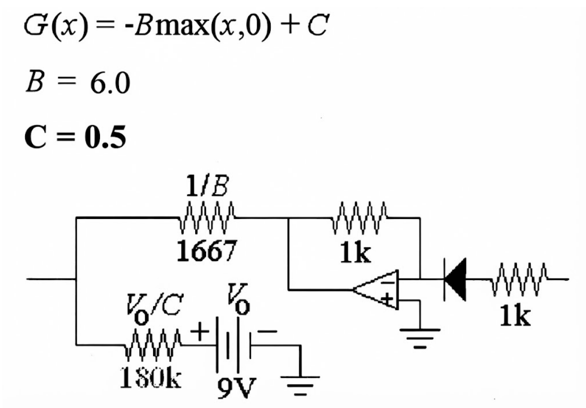

(a)

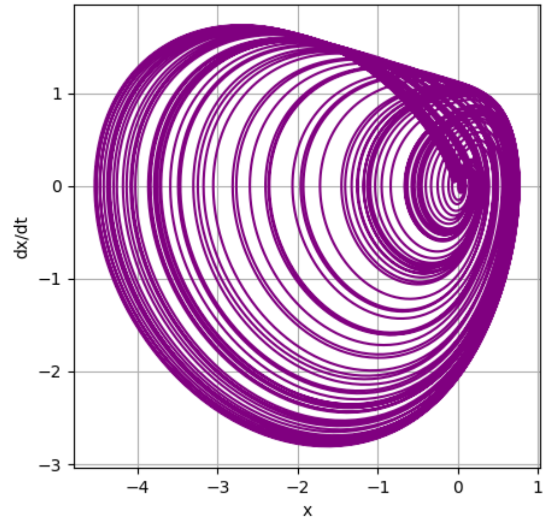

Figure 3: Python simulation of the chaotic attractor in the x–$\dot{x}$ plane for $G(x) = -B\max(x, 0) + C$.

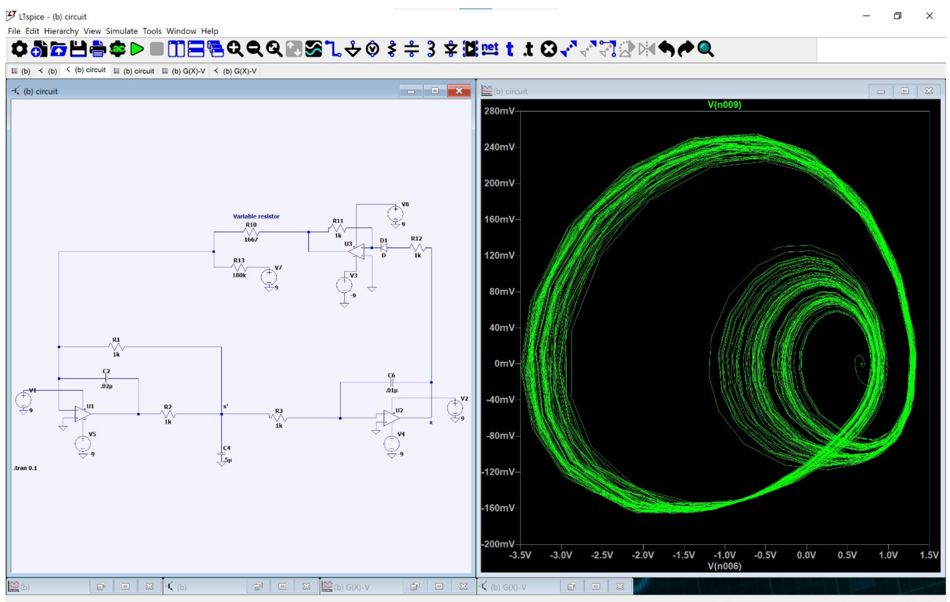

Figure 4: Transient simulation of the integrated chaotic circuit using the half-wave rectification configuration [circuit (b)], displaying the resulting phase portrait.

Testing resistor R_{10} at different values shows how it changes the circuit, as shown in Fig. 5. At a low resistance of $100\,\Omega$, the phase portrait stretches wide to $-13\,\text{V}$. At a medium resistance of $1500\,\Omega$, the attractor shrinks to a normal size. At a high resistance of $8\,\text{k}\Omega$, the chaotic pattern collapses into a tight spiral. This proves that adjusting R_{10} directly controls the size and stability of the chaos.

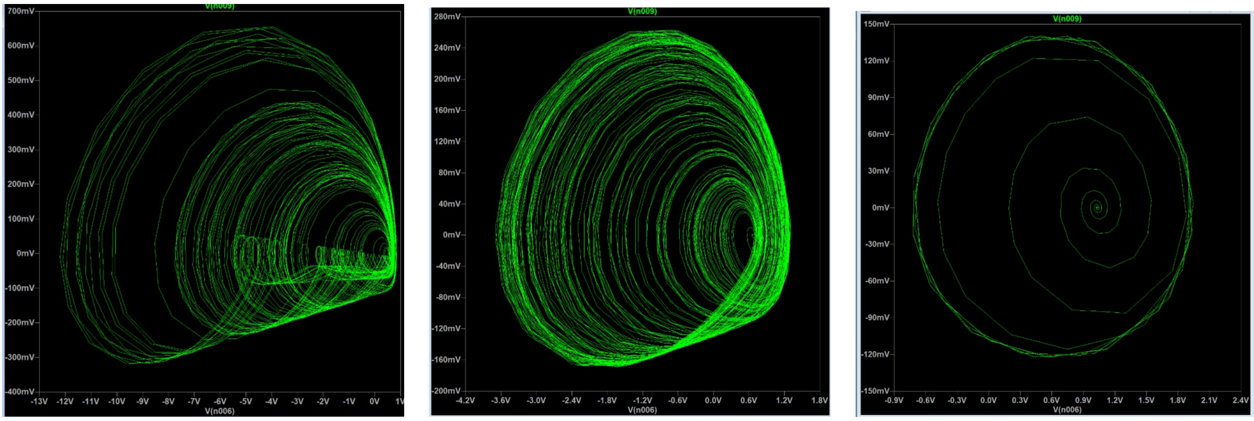

(a) Low resistance (b) Medium resistance (c) High resistance

Figure 5: Phase portrait variations observed during the resistance parameter sweep of R10.

Circuit (c): $G(x) = Bx - C\,\mathrm{sgn}(x)$

A single diode-free resistor $1/B$ ($8333\,\Omega$) connects the input to the output directly, providing a steady, smooth slope and contributing Bx for all x. A comparator-configured op-amp, powered from $\pm V_S$ ($9\,\mathrm{V}$), outputs $+V_S$ or $-V_S$ depending on the sign of x, driving resistor V_S/C ($20\,\mathrm{k}\Omega$) back into the input node and injecting $-C\,\mathrm{sgn}(x)$. Summing both branches:

$$G(x) = Bx - C\,\mathrm{sgn}(x). \tag{7}$$

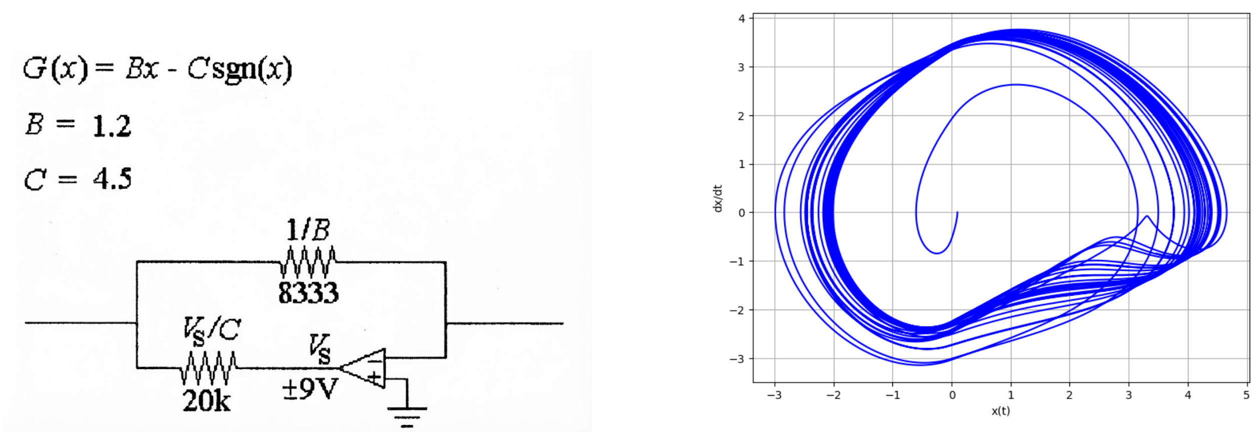

(a)

Figure 6: Python simulation of the chaotic attractor in the x–$\dot{x}$ plane for circuit (c) with $G(x) = Bx - C\,\mathrm{sgn}(x)$.

Circuit (d): $G(x) = -Bx + C\,\mathrm{sgn}(x)$

The same resistor network as circuit (c) utilizing $1/B = 8333\,\Omega$, $V_S/C = 45\,\mathrm{k}\Omega$ (here $C = 2.0$), is followed by an extra inverting unity-gain stage (an added op-amp with two $1\,\mathrm{k}\Omega$ resistors), which flips the sign of the entire network output:

$$G(x) = -\big[Bx - C\,\mathrm{sgn}(x)\big] = -Bx + C\,\mathrm{sgn}(x). \tag{8}$$

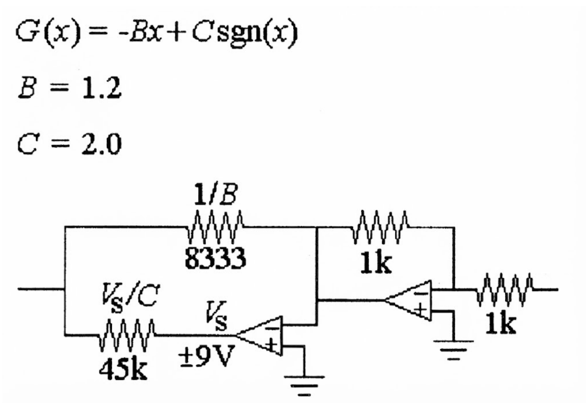

(a)

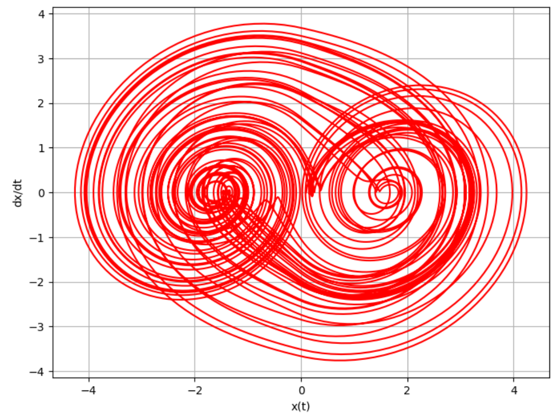

(b) Python simulation

Figure 7: Python simulation of the chaotic attractor in the x–$\dot{x}$ plane for circuit (d) with $G(x) = -Bx + C\,\mathrm{sgn}(x)$.

Fig. 8. shows the LTspice DC sweep validation for all four nonlinear G(x) circuits alongside their Python numerical simulations. The left column displays the LTspice circuit schematics with their output traces, while the right column shows the corresponding Python plots of the G(x) functions. Circuits (a) through (d) demonstrate the absolute value V-shape, half-wave rectifier, signum discontinuity at x=0, and inverted signum respectively. The close match between LTspice and Python results confirms that each circuit correctly implements its intended nonlinear function before integration into the full jerk system.

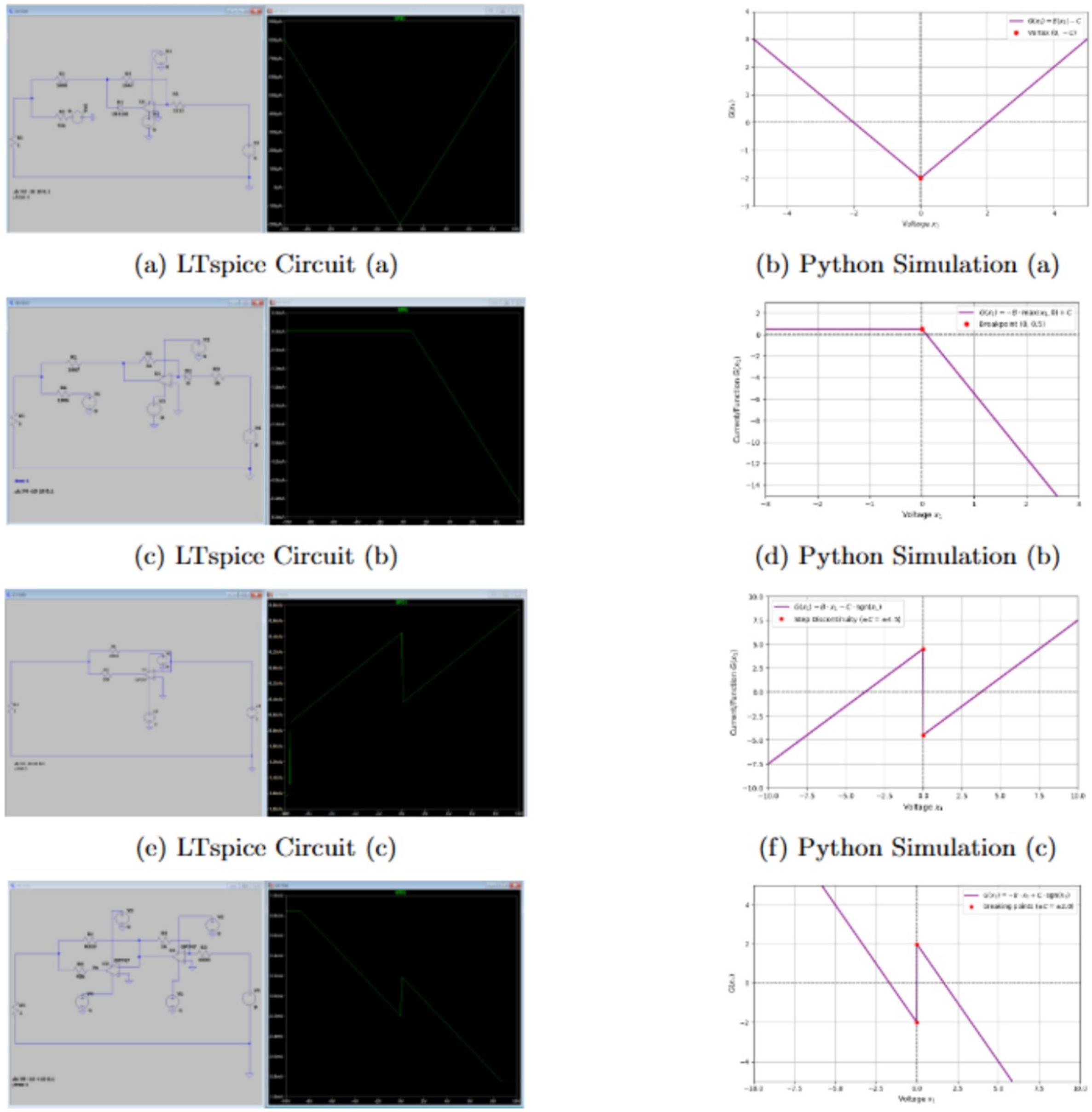

(a) LTspice Circuit (a) | (b) Python Simulation (a)

(c) LTspice Circuit (b) | (d) Python Simulation (b)

(e) LTspice Circuit (c) | (f) Python Simulation (c)

(g) LTspice Circuit (d) | (h) Python Simulation (d)

Figure 8: Comparison of LTspice DC sweep circuits (left column) and corresponding Python numerical simulations (right column) for circuits (a), (b), (c), and (d) in the x–$\dot{x}$ plane.

Beyond the four piecewise-linear circuits above, Sprott's Table 1 lists additional smooth nonlinearities that also yield chaos when substituted into Eq. (1) [1]. Numerical simulations for six such cases are shown in Fig. 9.

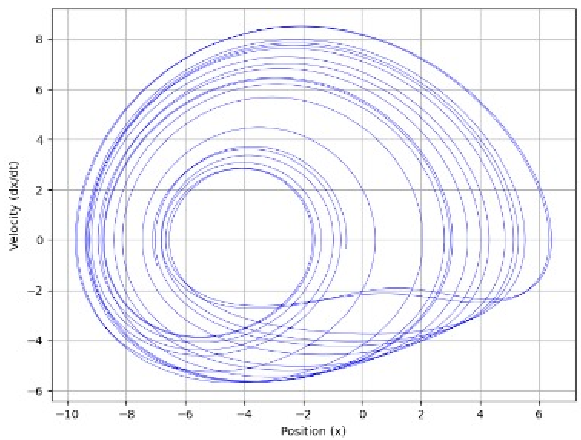

(a) Python simulation of the chaotic attractor in the position (x) versus velocity ($\dot{x}$) plane for the $G(x) = \pm B(x^2/C - C)$ configuration.

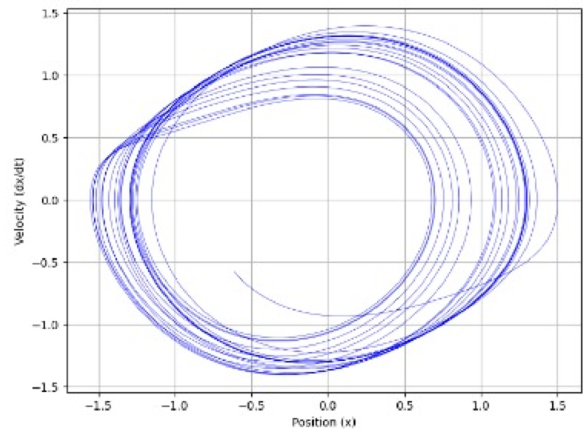

(b) Python simulation of the chaotic attractor in the position (x) versus velocity ($\dot{x}$) plane for the $G(x) = Bx(x^2/C - 1)$ configuration.

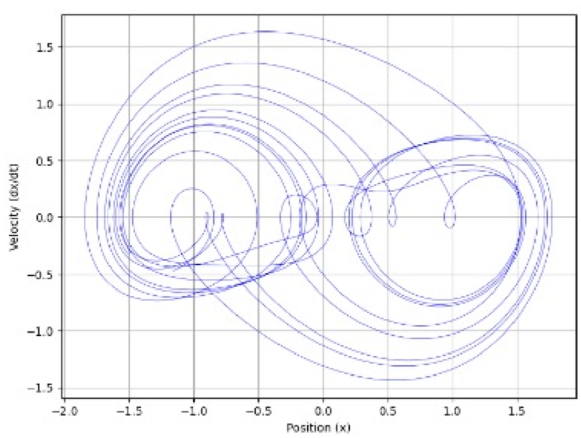

(c) Python simulation of the chaotic attractor in the position (x) versus velocity ($\dot{x}$) plane for the $G(x) = -Bx(x^2/C - 1)$ configuration.

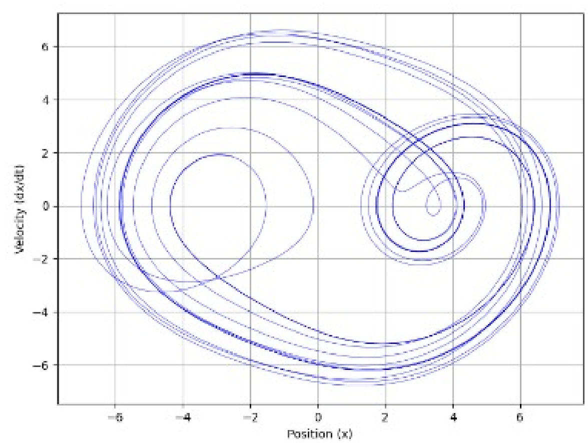

(d) Python simulation of the chaotic attractor in the position (x) versus velocity ($\dot{x}$) plane for the $G(x) = -B\left[x - \frac{2\tanh(Cx)}{C}\right]$ configuration.

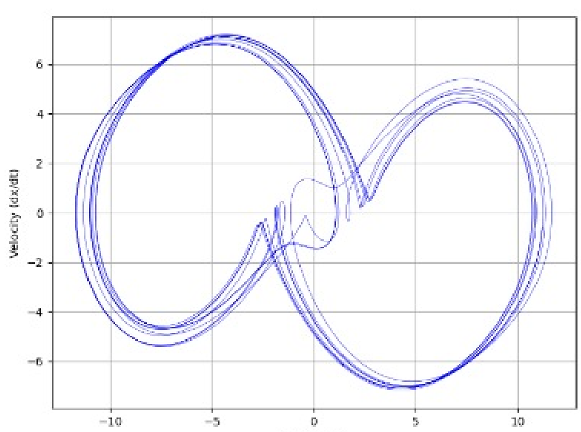

(e) Python simulation of the chaotic attractor in the position (x) versus velocity ($\dot{x}$) plane for the $G(x) = \pm\frac{B\sin(Cx)}{C}$ configuration.

6

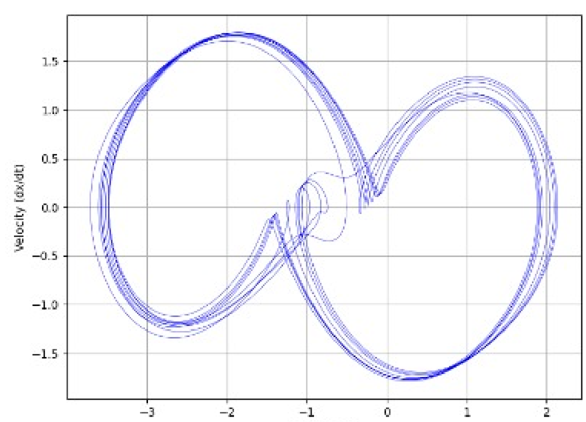

(f) Python simulation of the chaotic attractor in the position (x) versus velocity ($\dot{x}$) plane for the $G(x) = \pm\frac{B\cos(Cx)}{C}$ configuration.

Figure 9: Chaotic attractors produced by additional nonlinear functions $G(x)$ in the x–$\dot{x}$ phase plane.

Acknowledgments

The authors thank Dr. Muhammad Sabieh Anwar, Dr. Muhammad Hamza Humayun, Sir Faisal Saeed, and Sir Jamal Liaqat of PhysLab, LUMS, for their invaluable guidance and support throughout this project.

References

[1] J. C. Sprott, "A new class of chaotic circuit," *Physics Letters A*, vol. 266, no. 1, pp. 19–23, 2000.

[2] M. W. Hirsch, S. Smale, and R. L. Devaney, *Differential Equations, Dynamical Systems, and an Introduction to Chaos*, 2nd ed. Academic Press, 2004.

[3] H. P. W. Gottlieb, "What is the simplest jerk function that gives chaos?" *Am. J. Phys.*, vol. 64, no. 5, pp. 525–528, 1996.

[4] T. Matsumoto, L. O. Chua, and M. Komuro, "The double scroll," *IEEE Trans. Circuits Syst.*, vol. CAS-32, no. 8, pp. 797–818, 1985.

[5] T. Matsumoto, L. O. Chua, and M. Komuro, "Double scroll via a two-transistor circuit," *Physica D*, vol. 24, no. 1-3, pp. 97–113, 1987.

[6] S. J. Linz, "Nonlinear dynamical models and jerky motion," *Am. J. Phys.*, vol. 65, no. 6, pp. 523–526, 1997.

[7] S. J. Linz and J. C. Sprott, "Elementary chaotic flow," *Phys. Lett. A*, vol. 259, no. 3-4, pp. 240–243, 1999.

[8] O. E. Rössler, "An equation for continuous chaos," *Phys. Lett. A*, vol. 57, no. 5, pp. 397–398, 1976.

[9] R. J. Wincentsen, "Absolute value circuit," *EDN*, vol. 17, p. 44, Nov. 1972.

[10] P. Coullet, C. Tresser, and A. Arneodo, "Transition to stochasticity for a class of forced oscillators," *Phys. Lett. A*, vol. 72, no. 4-5, pp. 268–270, 1979.

[11] A. Arneodo, P. Coullet, and C. Tresser, "A possible new mechanism for the onset of turbulence," *Phys. Lett. A*, vol. 81, no. 4, pp. 197–201, 1981.

[12] N. F. Rul'kov, A. R. Volkovskii, A. Rodriguez-Lozano, E. Del Rio, and M. G. Velarde, "Mutual synchronization of chaotic self-oscillators with dissipative coupling," *Int. J. Bifurc. Chaos*, vol. 2, no. 3, pp. 669–676, 1992.

[13] E. Del Rio, M. G. Velarde, A. Rodriguez-Lozano, N. F. Rul'kov, and A. R. Volkovskii, "Experimental evidence in a nonlinear electronic circuit of the two types of chaotic behavior predicted by the manifold boundary crisis model," *Int. J. Bifurc. Chaos*, vol. 4, no. 5, pp. 1003–1009, 1994.

[14] J. Kaplan and J. Yorke, "Chaotic behavior of multidimensional difference equations," in *Functional Differential Equations and Approximation of Fixed Points*, H.-O. Peitgen and H.-O. Walther, Eds., Lecture Notes in Mathematics, vol. 730. Springer, 1979, pp. 204–227.